



Title	Word representation of streamline topologies for structurally stable vortex flows in multiply connected domains
Author(s)	Yokoyama, Tomoo; Sakajo, Takashi
Citation	Proceedings of the Royal Society A: Mathematical, Physical & Engineering Sciences, 469(2150), 20120558 https://doi.org/10.1098/rspa.2012.0558
Issue Date	2013-02-08
Doc URL	http://hdl.handle.net/2115/51916
Type	article (author version)
File Information	PRSA469-2150_20120558.pdf



[Instructions for use](#)

Word representation of streamline topologies for structurally stable vortex flows in multiply connected domains

Tomoo Yokoyama and Takashi Sakajo
Department of mathematics, Hokkaido University,
CREST, Japan Science and Technology Agency

November 15, 2012

Abstract

Let us consider the incompressible and inviscid flows in two-dimensional domains with multiple obstacles. The instantaneous velocity field becomes a Hamiltonian vector field defined from the stream function, and it is topologically characterized by the streamline pattern that correspond to the contour plot of the stream function. The present paper provides us with a procedure to construct structurally stable streamline patterns generated by finitely many point vortices in the presence of the uniform flow. Starting from some basic structurally stable streamline patterns in the disk of low genus, we repeat some fundamental operations that append a streamline pattern with increasing one genus to them. Thanks to the inductive procedure, one can assign a sequence of the operations as a representing word to each structurally stable streamline patterns. We also give the canonical expression for the word representation, which allows us to make a catalogue of all possible structurally stable streamline patterns in a combinatorial manner. As an example, we show all streamline patterns in the disk of genus one and two.

1 Introduction

Vortex structures in the presence of the uniform flow in exterior domains with multiple obstacles are observed in flow phenomena arising in environmental flows and biofluids. For instance, it is important to predict the diffusion of contaminants advected by the flow in rivers and ocean flows, in which the flow domain contains many obstacles such as waterbreaks, sandbanks and islands. Johnson and McDonald[8] considered the motion of vortices near multiple slit-shaped gaps to recognize the importance of the gaps in mid-ocean barriers to ocean circulations. They also studied the motion of a vortex near two cylindrical islands to understand how the topography of the flow domain affected the evolution of the vortex and thus they suggested that it played a significant role in the mass transporting in ocean flows[7]. In biofluids, it has been recognized numerically that interaction between the wings and the vortices shed from them realizes an efficient flight of butterflies[6] and a slow vertical descend of plant seeds[11].

As a mathematical model to deal with these problems, we consider incompressible and inviscid flows in multiply connected domains. We impose the slip boundary condition to the flow along the boundaries of the domain. The inviscid model remains valid for the slightly viscous flows unless the flow is highly turbulent, since point vortices can approximate the vortex structures shed from the boundaries owing to the formation of thin boundary layers. Moreover, the model has a theoretical advantage thanks to its mathematical simplicity. That is to say, when we identify the two-dimensional space $(x, y) \in \mathbb{R}^2$ with the complex plane $z = x + iy \in \mathbb{C}$, the inviscid flow in the two-dimensional space is represented by an analytic function called *the complex potential*, say $F(z)$, from which the two-dimensional velocity field (u, v) is recovered owing to the formula $u - iv = F'(z)$. The imaginary part of the complex potential $\psi(z) = \text{Im}[F(z)]$, which is known as *the stream function*, also has a significant physical meaning, since a contour line of this function is identical to a streamline of the flow. In addition, the motion of a particle located at $(x_0(t), y_0(t))$ at time t is described by $\frac{dx_0}{dt} = \frac{\partial \psi}{\partial y}$ and $\frac{dy_0}{dt} = -\frac{\partial \psi}{\partial x}$, which indicates that $\psi(z)$ gives rise to a Hamiltonian vector field for the particle evolution.

Complex potentials for a given multiply connected domain are obtained from those for a canonical multiply connected domain with the same multiplicity by constructing the conformal mapping between these two domains, since the complex potentials are conformally invariant. Crowdy and Marshall[4] considered a domain in the unit circle that contains many circular boundaries, called a *circular domain*, for which the analytic formulae of the complex potential for a point vortex has been provided. The complex potential for the uniform flow in exterior circular domains has also been constructed by Crowdy[3]. These complex potentials are described in terms of a transcendental function, called *the Schottky-Klein prime function*, that is defined associated with the radii and centers of the circular boundaries.

In view of the applications to the fluid problems stated above, we are interested in the potential flows generated by many point vortices in multiply connected exterior domains in the presence of the uniform flow, which we refer to as *vortex flows*. In particular, in the present paper, we are concerned with the global topological structure of the streamline patterns generated by vortex flows and then we classify them in a unified manner. The importance of topological studies of irrotational flows has already been realized by Klein[9]. Furthermore, among all possible streamlines, we focus on *structurally stable* vortex flows. The structural stability here means that the qualitative behavior of the streamlines is unchanged under small continuous perturbations, whose exact definition will be provided in the following section. The structurally stable flows are also physically significant since they are more likely to be observed in many real fluid flows. Topological classification of the streamline patterns has been investigated for the vortex flows in the unbounded plane without boundaries[1] and on a sphere[10], although the uniform flow was not contained in these studies. The present paper is not only an extension of the preceding works to the vortex flows in multiply connected domains, but it also has a theoretical significance because of the following three reasons. First, the uniform flow adds a new streamline structure to the flow, which has not been considered so far. Second, owing to the existence of boundaries in the domain, we need to consider a streamline attached to these boundaries that give rise to another structurally stable streamline pattern. Finally, even though we restrict our attention to the structurally stable velocity field, we obtain many non-trivial streamline patterns, since it has been shown that homoclinic connections generated by the divergence-free vector field on 2D manifold are structurally stable[12]. Consequently, the structurally stable streamline patterns generated by the vortex flows with the uniform flow in multiply connected domains can have various topological patterns, whose classification provides us with a significant catalogue of flow patterns arising in biofluids and environmental flows.

Construction of the streamline patterns proceeds as follows. Starting from some basic structurally stable flow patterns in the disk of low genus, we obtain the flow patterns in the multiply connected domain with higher genus by repeating fundamental operations that append a structurally stable streamline pattern with increasing one genus in the domain. Accordingly, one can assign a sequence of the operations for a streamline pattern, which we call a *word representation of the streamline pattern*. Thanks to the word representation, we can make a catalogue of all possible structurally stable streamline patterns generated by the vortex flows in a combinatorial way.

This paper consists of five sections. In the next section, after reviewing some known results on the complex potentials for a point vortex and the uniform flow in multiply connected circular domains, we give two streamline patterns in the disk of genus zero and one pattern in the annulus of genus one. We show that they are only structurally stable streamline patterns to which the construction procedure is applied. In §3, we introduce five fundamental operations that add a structurally stable streamline pattern with one genus to the flow, with which we show how to construct streamline patterns in multiply connected domains with higher genus and how to assign their word representations. In §4, applying the construction procedure, we give all possible structurally stable streamline topologies and their word representation generated by the vortex flows in multiply connected domains of genus 1 and 2. The last section is summary and discussion.

2 Structurally stable vortex flows in multiply connected domains

Let us review some known results on the complex potentials in multiply connected domains. Suppose that a circular domain, say $\mathcal{D}_\zeta(M)$, in the unit circle of the complex ζ -plane contains M circular boundaries.

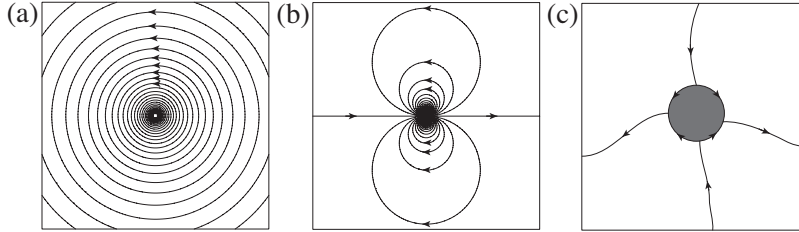


Figure 1: Schematic pictures of locally structurally stable streamline patterns. (a) Closed circular orbits around a point vortex. (b) Streamlines in the neighborhood of a 1-source-sink pair. (c) 4-saddle points at the boundary.

Then one can introduce a transcendental function $\omega(\zeta, \alpha)$ for $\zeta, \alpha \in \mathcal{D}_\zeta(M)$ as follows:

$$\omega(\zeta, \alpha) = (\zeta - \alpha) \prod_{\theta \in \Theta''} \frac{(\theta(\zeta) - \alpha)(\theta(\alpha) - \zeta)}{(\theta(\zeta) - \zeta)(\theta(\alpha) - \alpha)},$$

in which Θ'' denotes an infinite set of Möbius maps defined from the radii and the centers of the circular boundaries. See the paper[4, 5] for its detailed definition and properties.

Crowdy and Marshall[4] have provided with the analytic formulae of the complex potential $W_V(\zeta; \alpha_V)$ for a point vortex located at $\alpha_V \in \mathcal{D}_\zeta(M)$ with the strength κ , which is represented by

$$W_V(\zeta; \alpha_V) = \frac{\kappa}{2\pi i} \log \left(\frac{\omega(\zeta, \alpha_V)}{|\alpha_V| \omega(\zeta, \bar{\alpha}_V)} \right) \equiv \frac{\kappa}{2\pi i} W_0(\zeta; \alpha_V).$$

Since $W_0(\zeta; \alpha_V) \sim \log(\zeta - \alpha_V)$ as $\zeta \rightarrow \alpha_V$, the complex potential generates infinite circular closed streamlines in the neighborhood of the point vortex as we see in Figure 1(a). Note that as long as we are concerned with the topological structures of the streamlines, an elliptic center and a circular boundary cannot be distinguished from a point vortex, since the circular closed streamlines around them are topologically equivalent to those around a point vortex.

Let $\mathcal{D}_z(M)$ denote an exterior multiply connected domain with $M+1$ circular boundaries in the complex z -plane. Then the complex potential for the uniform flow in the domain is obtained from a complex potential function in the circular domain $\mathcal{D}_\zeta(M)$ by constructing a conformal mapping $z = g(\zeta)$ from $\mathcal{D}_\zeta(M)$ to $\mathcal{D}_z(M)$. Since $\mathcal{D}_z(M)$ is unbounded, the conformal mapping $g(z)$ maps some point in $\mathcal{D}_\zeta(M)$, say $\zeta = \beta_U$, to infinity of $\mathcal{D}_z(M)$. Thus the conformal mapping has the following form.

$$z = g(\zeta) = \frac{a}{\zeta - \beta_U} + \mathcal{O}(1), \quad \zeta \rightarrow \beta_U,$$

with a real constant a . Crowdy[3] showed that the complex potential $W_U(g^{-1}(z); \beta_U)$ gave the uniform flow with speed U and the inclined angle to the real axis ϕ of the complex z -plane, in which

$$W_U(\zeta; \beta_U) = Ua \left[e^{i\phi} \frac{\partial}{\partial \bar{\beta}} - e^{-i\phi} \frac{\partial}{\partial \beta} \right] W_0(\zeta, \beta) \Big|_{\beta=\beta_U}.$$

Since the uniform flow $W_U(g^{-1}(z); \beta_U)$ is analytic everywhere in $\mathcal{D}_z(M)$ except at infinity, it is represented by $W_U(g^{-1}(z); \beta_U) \sim Ue^{-i\phi}z + \mathcal{O}(1)$ as $z \rightarrow \infty$. Since we are just interested in the topological structure of the streamlines, we may assume that $\phi = 0$ and $\beta_U = 0$ without loss of generality. Thus the complex potential $W_U(\zeta; 0)$ behaves asymptotically as $W_U(\zeta; 0) \sim \frac{Ua}{\zeta} + \mathcal{O}(1)$ as $\zeta \rightarrow 0$. Since the leading singular term $\frac{1}{\zeta}$ represents the complex potential for a source-sink pair at the origin, the streamlines in the neighborhood of the source-sink pair correspond to the contour lines of the stream function $\text{Im}[1/\zeta] = -\frac{1}{r} \sin \theta$ in the polar coordinates (r, θ) around the origin, which consists of infinite orbits departing from and return to the source-sink pair as we see in Figure 1(b). Generally, the complex potential $\frac{1}{\zeta^n}$ ($n \geq 1$) gives rise to the flow of n -tuple source-sink pair located at the origin, whose stream function is given by $\text{Im}[1/\zeta^n] = -\frac{1}{r^n} \sin n\theta$

in the polar coordinates. Thus we can generalize the definition of the complex potential for the n -tuple source-sink pair in the multiply connected circular domains $\mathcal{D}_\zeta(M)$ as follows.

Definition 2.1. A point $p \in \mathcal{D}_\zeta(M)$ is said to be an n -source-sink point, if $V|_{\mathcal{D}_\zeta(M) \setminus \{p\}}$ is a vector field on $\mathcal{D}_\zeta(M) \setminus \{p\}$ generated by a stream function is denoted by ψ , for which there is a pair of a neighborhood U of p and a homeomorphism h from U to the unit disk D with $h(p) = 0$ such that $\psi \circ h^{-1}|_{D \setminus \{0\}} = -\frac{\sin n\theta}{r^n}$ in the polar coordinates associated with the disk D .

For the sake of later reference, we call that $h^{-1}(D) \subset \mathcal{D}_\zeta(M)$ is a standard disk. It is easy to see that the complex potential $W_U(\zeta, 0)$ gives the 1-source-sink point located at the origin of $\mathcal{D}_\zeta(M)$. Strictly speaking, since the set of streamlines converging to the n -source-sink point has a non empty interior point, it is unable to define a Hamiltonian vector field at this point, which requires us to loosen the definition of Hamiltonian vector fields. Thus, we say a vector field V is a Hamiltonian vector field with the n -source-sink point p , if $V|_{\mathcal{D}_\zeta(M) \setminus \{p\}}$ is a Hamiltonian vector field on $\mathcal{D}_\zeta(M) \setminus \{p\}$. Hence, in order to discuss the stability of the streamline topologies of the Hamiltonian vector fields with the n -source-sink point on $\mathcal{D}_\zeta(M)$, we need to give the exact definition of their structural stability. Denote by χ_n^r the set of C^r Hamiltonian vector fields with an n -source-sink point on $\mathcal{D}_\zeta(M)$ with C^r -topology ($r \geq 1$). Then we have the following definitions on the stability of the vector field in χ_n^r .

Definition 2.2. For $s \leq r$, $V \in \chi_n^r$ is locally (C^s)-structurally stable at $p \in \mathcal{D}_\zeta(M)$ in χ_n^r , if for any neighborhood U of p and any Hamiltonian vector field \tilde{V} , which is C^s -near of V in χ_n^r , \tilde{V} is topologically equivalent to V . In other words, there is a homeomorphism $h : U \rightarrow h(U) \subset \mathcal{D}_\zeta(M)$ such that h maps each orbit of $V|_U$ to that of \tilde{V} homeomorphically and it preserves the orientation of the orbits.

Definition 2.3. $V \in \chi_n^r$ is (C^1)-structurally stable, if any vector field \tilde{V} , which is C^1 -near of V in χ_n^r , is topologically equivalent to V .

Let us note that we use the standard definition of the structurally stability for the C^r -Hamiltonian vector field, denoted by \mathcal{H}^r , without the n -source-sink point as will be stated in Theorem 3.1. With these definitions, we prove the following proposition, which assures the structural stability in the neighborhood of the n -source-sink point locally in $\mathcal{D}_\zeta(M)$.

Proposition 2.1. For $r \geq 1$, $V \in \chi_n^r$ is locally structurally stable at the n -source-sink point p .

Proof. Let H be a Hamiltonian of V on $\mathcal{D}_\zeta(M) \setminus \{p\}$ and D_h a standard disk for p . Each streamline of V except p corresponds to a level set of H and it connects between either p and the boundary of D_h , or p and itself in $D_h \setminus \{p\}$. Since p is the n -source-sink point and its stream function is represented by $\text{Im} \left[\frac{1}{r^n} \right]$ in its neighborhood, the absolute value of the gradient of the Hamiltonian is strictly positive, i.e. $|\nabla H| \geq n > 0$ in $D_h \setminus \{p\}$. Hence, even if the vector field V is perturbed, $|\nabla \tilde{H}| > 0$ holds in $D_h \setminus \{\tilde{p}\}$ for its perturbed Hamiltonian \tilde{H} and the perturbed n -source-sink point \tilde{p} . Therefore there are a small neighborhood \tilde{D}_h of \tilde{p} and a topological equivalence $h : (D_h, p) \rightarrow (\tilde{D}_h, \tilde{p})$ such that $h|_{D_h \setminus \{p\}}$ maps V to the Hamiltonian vector field of $\tilde{H} \in \chi_n^r$. \square

It is easy to see that the flows around a point vortex, an elliptic center and a circular boundary are locally structurally stable in \mathcal{H}^r and χ_n^r . There is another different structurally stable streamline pattern in the neighborhood of the boundary, which consists of the streamlines connected to $2n$ saddle points at the boundary for $n \geq 1$ as in Figure 1(c).

We consider the complex potential $W(\zeta)$ in circular domain $\mathcal{D}_\zeta(M)$ that consists of the 1-source-sink point at the origin and N point vortices as follows.

$$W(\zeta) = W_U(\zeta; 0) + \sum_{m=1}^N \frac{\kappa_m}{2\pi i} W_0(\zeta; \alpha_m), \quad (1)$$

in which α_m denotes the location of the m th point vortex with strength κ_m . One can add the complex potential generating the circulation around the boundary, whose analytic formulae has also been provided by Crowdy[3]. However, it is unnecessary to consider the complex potential, since it just generates closed

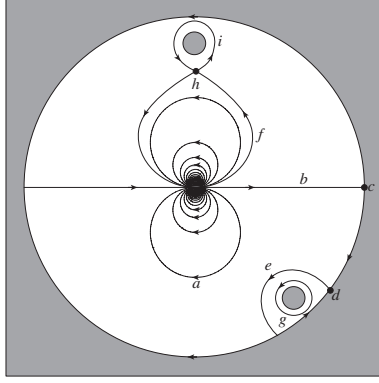


Figure 2: Schematic pictures of orbits. (a) ss -orbit; (b) ss - ∂ -saddle connection; (c) ss - ∂ -saddle; (d) ∂ -saddle; (e) ∂ -saddle connection; (f) ss -saddle connection; (g) closed orbit; (h) saddle point; (i) homoclinic saddle connection.

orbits around the boundary that are topologically equivalent to those generated by a point vortex and thus it adds no new topological streamline structure to the flow.

We are interested in the global topology of structurally stable streamline patterns of the flow generated by the complex potential (1). The genus M of the flow domain $\mathcal{D}_\zeta(M)$ is equivalent to the sum of the numbers of elliptic centers, point vortices and circular boundaries contained in the domain. However, for the sake of simplicity, we regard M as the number of circular boundaries when considering streamline patterns, since closed circular orbits around an elliptic center or a point vortex are topologically indistinguishable from those around a circular boundary. Let us also note that it is sufficient to classify the streamline topologies in the bounded circular domain $\mathcal{D}_\zeta(M)$, since it can be mapped to an exterior domain $\mathcal{D}_z(M)$ by a conformal mapping and the streamline patterns generated by $W(\zeta)$ are kept unchanged topologically under the action of the conformal mapping.

For the sake of reference, we name all components of the structurally stable streamlines generated by the complex potential $W(\zeta)$ in the multiply connected domain $\mathcal{D}_\zeta(M)$. See Figure 2. Streamlines departing from and return to the 1-source-sink point are called ss -orbits. When an orbit connects between the 1-source-sink point and a saddle point at the boundary, we refer to the orbit and the saddle point as an ss - ∂ -saddle connection and an ss - ∂ -saddle. A ∂ -saddle is a saddle at the boundary that is not connected to the 1-source-sink point. If two ∂ -saddles are connected by a streamline, we say the connecting orbit a ∂ -saddle connection. A streamline connecting a saddle point with the 1-source-sink point is called an ss -saddle connection. The other orbits consist of circular closed orbits, saddles and their homoclinic saddle connections.

Since we construct the structurally stable streamline patterns in $\mathcal{D}_\zeta(M)$ from those in $\mathcal{D}_\zeta(M - 1)$ inductively as will be explained in the next section, we need initial streamline patterns. There are two fundamental streamline patterns in $\mathcal{D}_\zeta(0)$, both of which contain the 1-source-sink point at the origin. The first pattern in Figure 3(a) contains two ss - ∂ -saddles that are connected to the 1-source-sink point via ss - ∂ -saddle connections, whose streamline topology is denoted by I . In the second pattern, there contains no ss - ∂ -saddle connection but one saddle point with a homoclinic saddle connection and two ss -saddle connections as shown in Figure 3(b), which is symbolized by II . Recall that the closed disk has the Euler number 1, the indices of an n -source-sink point, a saddle and a ∂ -saddle are $2n$, -1 and $-1/2$ respectively and that the Euler number equals to the sum of indices of (∂ -)saddles by Poincaré-Hopf theorem. Then it is easy to show that I and II are the only structurally stable streamline patterns in $\mathcal{D}_\zeta(0)$, since we have either one saddle or two ∂ -saddles to satisfy Poincaré-Hopf theorem. In terms of the equality of the indices, the streamline patterns I and II correspond to $1 = 2 + (-1)$ and $1 = 2 + 2 \cdot (-1/2)$ respectively. The streamline patterns I and II are substantially different in a mathematical sense that they cannot be transformed to each other continuously. In the circular domain $\mathcal{D}_\zeta(1)$, we have one initial structurally stable streamline pattern that cannot be constructed from the patterns I and II . The streamline pattern is denoted by O that consists of regular closed orbits around the circular boundary as in Figure 3(c). The

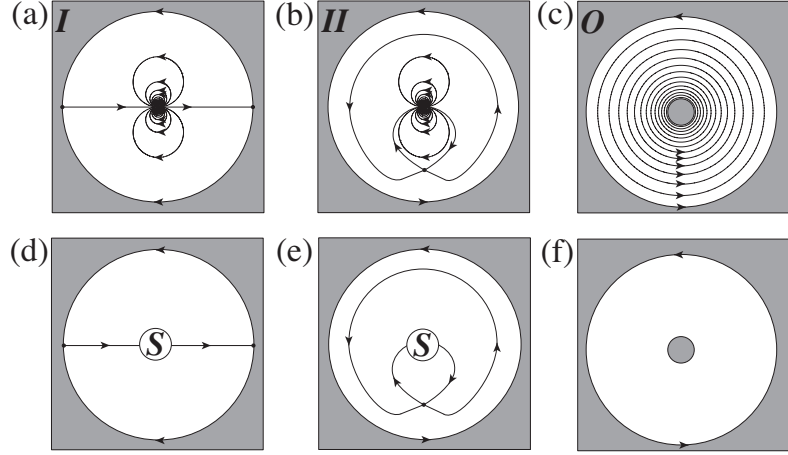


Figure 3: Fundamental structurally stable streamline patterns with the 1-source-sink point in $\mathcal{D}_\zeta(0)$. (a) Pattern *I* with two ss - ∂ -saddle connections; (b) Pattern *II* with a saddle connected by a homoclinic saddle point and two ss -saddle connections. Their topological structures are schematically shown by (d) and (e) respectively, in which the 1-source-sink point is symbolized by \textcircled{S} and no ss -orbits are drawn. (c) Fundamental structurally stable streamline pattern in $\mathcal{D}_\zeta(1)$ without the 1-source-sink point, which is schematically shown by (f), in which no closed orbit is drawn.

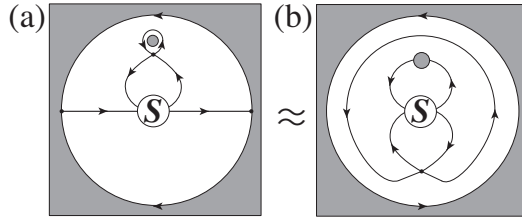


Figure 4: Equivalent streamline topologies in $\mathcal{D}_\zeta(1)$. In terms of the word representation introduced later, the equivalence is denoted by $IA_0 = IIA_2$.

streamline patterns *I* and *II* (resp. *O*) are the initial structurally stable patterns in χ_n^r (resp. \mathcal{H}^r) to which we apply the procedure to construct streamline patterns in multiply connected domains with higher genus. In what follows, for the sake of simplicity to draw streamline patterns, we show no ss -orbits and closed orbits, but we pay attention to the global topological structure of ss - ∂ -saddle connections, ∂ -saddle connections, homoclinic saddle connections and ss -saddle connections, since these orbits are substantial to distinguish the streamline topologies. In addition, the 1-source-sink point is schematically symbolized by \textcircled{S} as we see Figure 3(d) and (e).

Let us finally note that a topological equivalence between two streamline patterns. Figure 4 shows two equivalent patterns in $\mathcal{D}_\zeta(1)$. They consist of the 1-source-sink point with two ss - ∂ -saddle connections and one saddle point with a homoclinic saddle connection and two ss -saddle connections. They look different at a glance, but they have the same topological structure, if we identify the outer boundary of Figure 4(a) with the inner boundary of Figure 4(b) and vice versa. In other words, there is a homeomorphism of a closed annulus exchanging the boundaries which maps (a) to (b). In the topological classification of streamline patterns, these two patterns are identified as one pattern. This fact plays an important role in assigning words for streamline patterns.

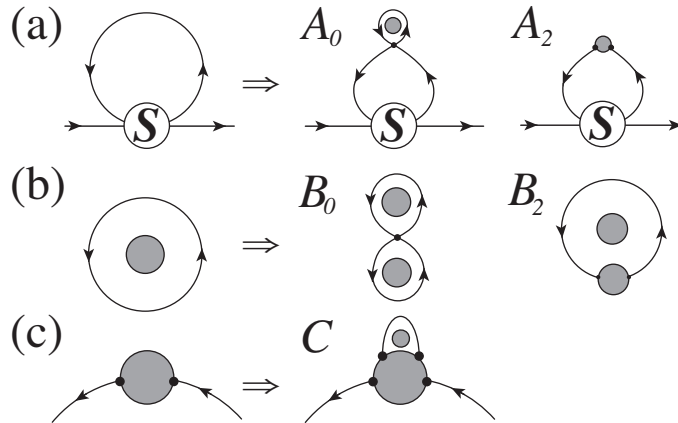


Figure 5: Five operations to construct structurally stable streamline patterns with adding one genus to the domain. (a) The operations A_0 and A_2 on an ss-orbit; (b) the operations B_0 and B_2 on a closed orbit; (c) the operation C on a boundary with ∂ -saddles.

3 Word representation of streamline topologies

We introduce the following five operations to build up structurally stable streamline patterns in $\mathcal{D}_\zeta(M)$ from those in $\mathcal{D}_\zeta(M-1)$ by adding one genus to the domain. Schematic pictures for these operations are shown in Figure 5.

- (A_0) An ss-orbit is replaced by a saddle with a homoclinic saddle connection enclosing a circular boundary, and two ss-saddle connections.
- (A_2) An ss-orbit is replaced by two ∂ -saddles at a circular boundary that connect to the 1-source-sink pair with two ss- ∂ -saddle connections.
- (B_0) A closed orbit is replaced by a saddle with two homoclinic saddle connections, i.e., a figure eight saddle-connection.
- (B_2) A closed orbit is replaced by two ∂ -saddles at a circular boundary connected by a ∂ -saddle connection.
- (C) Two ∂ -saddles with a ∂ -saddle connection are added to a circular boundary equipped with $2k$ ∂ -saddles ($k > 0$). The ∂ -saddle connection and the boundary enclose a circular boundary.

The operations A_0 and A_2 can be applied to ss-orbits, while B_0 and B_2 are done to closed orbits. The operation C cannot be applied to boundaries without ∂ -saddles. We shall prove later that these are the only operations by which we obtain the structurally stable streamline patterns from the initial patterns O , I and II .

First, we construct structurally stable streamline patterns without the 1-source-sink point starting from the initial pattern O in Figure 3(f) by applying the operations defined above repeatedly. Since the flow contains no 1-source-sink point, it is sufficient to recall the characterization of structural stability for Hamiltonian vector fields on a two dimensional compact submanifold of a closed orientable connected surface[12].

Theorem 3.1 (Theorem 2.3.8. p.74 [12]). *Suppose that V is a C^r -Hamiltonian vector field on a compact orientable surface. V is structurally stable in \mathcal{H}^r , if and only if V is regular and all (∂ -)saddle connections are self-connected.*

In addition, it is well known that any divergence-free vector field is determined by the union of saddle connections and the ∂ -saddle connections, called the *saddle connection diagram*, up to topological equivalence[12]. The operations A_0 and A_2 are unable to be applied to the pattern O , since it never contains the 1-source-sink point and thus no ss-orbits. Hence, we assign a sequence of the operations, say

$OO_1O_2\cdots O_k$ with $O_i \in \{B_0, B_2, C\}$ for $i = 1, \dots, k$, as a representing word of the streamline pattern. We now prove that B_0 , B_2 and C are the only operations in order to construct structurally stable streamline patterns from O .

Corollary 3.1. *Suppose that the Hamiltonian vector field V is structurally stable in \mathcal{H}^r . Then V can be represented by a sequence of the operations starting from the initial pattern O .*

Proof. By Theorem 3.1, the saddle connection diagram consists of homoclinic saddle connections and ∂ -saddle connections that connect two ∂ -saddles at the same boundary. Recall that the Euler number of $\mathcal{D}_\zeta(M)$ is $1 - M$. Since V is regular, we can suppose that there are k_1 saddles and k_2 ∂ -saddles. By Poincaré-Hopf theorem, these numbers satisfy $M - 1 = k_1 + k_2/2$.

We will show the assertion by induction on M . Suppose that $M = 1$. Then $k_1 = k_2 = 0$ and so there are no saddles and ∂ -saddles. Hence V is regular and we have O . Suppose that $M > 1$. We say that a connected component in the saddle connection diagram is inner most, if it bounds no other saddles and ∂ -saddles. If an inner most component in the saddle connection diagram of V in $\mathcal{D}_\zeta(M)$ is a homoclinic saddle connection (resp. a ∂ -saddle connection with two ∂ -saddles), then V is obtained by the operation B_0 (resp. B_2) from a structurally stable Hamiltonian vector field \tilde{V} on $\mathcal{D}_\zeta(M - 1)$. By inductive hypothesis, suppose that \tilde{V} is represented by $OO_1\cdots O_{M-2}$, then V has a word representation $OO_1\cdots O_{M-2}B_0$ (resp. $OO_1\cdots O_{M-2}B_2$). Otherwise all inner most components are ∂ -saddle connections with more than two ∂ -saddles. Then V is obtained by the operation C from a structurally stable Hamiltonian vector field \tilde{V} on $\mathcal{D}_\zeta(M - 1)$. Hence, V has a word representation $OO_1\cdots O_{M-2}C$. \square

We must notice that there must be B_2 before C appears in the sequence of operations, since the pattern O has no ∂ -saddles and thus C can only be applied to a boundary with ∂ -saddles that is created as a result of B_2 . Hence we have the following lemma.

Lemma 3.1. *Let $OO_1\cdots O_{M-1}$ be a sequence of operations, where $O_i \in \{B_0, B_2, C\}$. Then the followings are equivalent.*

- 1) *The sequence is a word representation for a structurally stable Hamiltonian vector field in $\mathcal{D}_\zeta(M)$.*
- 2) *For any i with $O_i = C$, there is some $j < i$ such that $O_j = B_2$.*

We call the sequence of operations an O -word for a given structurally stable Hamiltonian vector field. According to Lemma 3.1, either B_0 or B_2 can follow the initial word O . Hence, the structurally stable streamline patterns in $\mathcal{D}_\zeta(2)$ are OB_0 and OB_2 , whose saddle connection diagrams are shown in Figure 6(a) and (c) respectively.

Now, we consider the structurally stable streamline patterns with the 1-source-sink point constructed from the initial patterns I and II . We need to modify the structural stability of the Hamiltonian vector field due to the existence of the 1-source-sink point V in $\mathcal{D}_\zeta(M)$. In order to do this, let us first note how to characterize streamline patterns I and II generated by the 1-source-sink point. The saddle connection diagram for OB_0 shown in Figure 6(a) is topologically equivalent to that shown in Figure 6(b) for the same reason as we discussed in Figure 4. Then replacing the two circular obstacles by two center points and collapsing these centers to one point on the homoclinic orbit between them, we obtain the streamline pattern II . In the similar manner, there is a homeomorphism of OB_2 exchanging the boundaries which maps (c) to (d). Thus the streamline pattern I is obtained by collapsing two centers to one point on the ∂ -saddle connection in the middle. Accordingly, the streamline patterns I and II are constructed from the singular pattern OB_2 and OB_0 by identifying two centers to one point, which is the location of the 1-source-sink point.

The structural stability for the Hamiltonian vector fields with the 1-source-sink point is characterized as follows.

Theorem 3.2. *The Hamiltonian vector field $V \in \chi_1^r$ is structurally stable, if and only if*

- (1) *the restriction of V on the complement of the 1-source-sink point is regular,*
- (2) *all saddle connections are homoclinic connections,*
- (3) *all ∂ -saddle connections connect two ∂ -saddles located at the same boundary.*

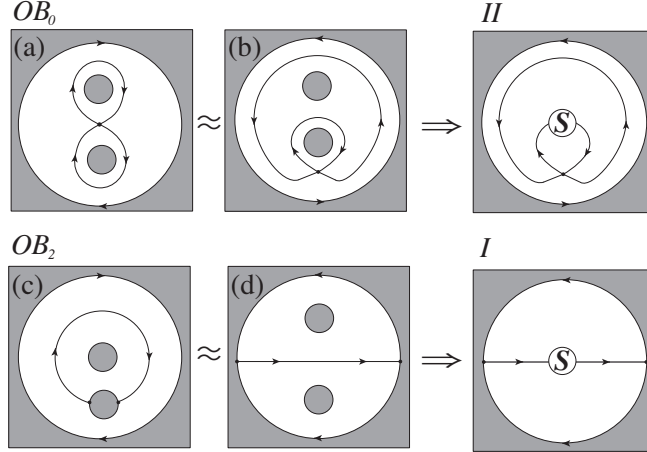


Figure 6: (a),(b) saddle connection diagrams represented by OB_0 and (c),(d) saddle connection diagrams represented by OB_2 . It shows how to construct the streamline pattern II from OB_0 (resp. I from OB_2); Collapsing the two centers in OB_0 (resp. OB_2) to one point on the homoclinic connection (resp. on the ∂ -saddle connection), we obtain the streamline pattern II (resp. I).

Proof. Obviously the regularity is necessary. Therefore we may assume that the restriction of V on the complement of the 1-source-sink point p is regular. Now suppose that there is a heteroclinic saddle connection between two distinct saddles p and q . Then $H(p) = H(q)$ is satisfied where H represents the Hamiltonian for $V \in \chi_1^r$. We will show that the energy equality does not hold when we perturb the vector field. In order to accomplish it, we introduce a Hamiltonian vector field as follows. Let $b : [0, 1] \rightarrow [0, 1]$ be a smooth non-increasing function such that $b(r) = 1$ for $r \in [0, 1/3]$, $b(r) = 0$ for $r \in [2/3, 1]$, $b'(r) < 0$ for $r \in (1/3, 2/3)$, with which we define an axisymmetric function $f : U \rightarrow [0, 1]$ by $f(r, \theta) := b(r)$ in the polar coordinates (r, θ) of the unit disc U . Let V_f be a Hamiltonian vector field on U defined from f . Then, a contour line of $f(r, \theta)$ for any $r \in (1/3, 2/3)$ is a closed orbit. For arbitrary $\varepsilon > 0$, we define a function \tilde{H} on $\mathcal{D}_\zeta(M)$ by $\tilde{H} := H + \varepsilon f$ on the open unit disc U around p and $\tilde{H} := H$ otherwise. Then \tilde{H} is a smooth function and so define the Hamiltonian vector field \tilde{V} . Since $\tilde{H}(p) - \tilde{H}(q) = H(p) + \varepsilon f(p) - H(q) = \varepsilon \neq 0$, there is no orbits connecting p and q . Hence V is not structurally stable.

If there is a ∂ -saddle connection between two ∂ -saddles p and q at different boundaries with the same energy level $H(p) = H(q)$. Then we can show the vector field V is not structurally stable as follows. Considering an annulus $[0, 1) \times S^1$ in $[0, \infty) \times S^2$ around the circular boundary with p , we can define the perturbed Hamiltonian vector field \tilde{H} obtained from H by perturbing it in the annulus with using the function $b(r)$, for which the energy equality no longer holds.

Conversely, suppose that (1), (2) and (3) hold. By Proposition 2.1, V is locally structurally stable at the 1-source-sink point. Let \tilde{V} be a small perturbed vector field of V . Then we may assume that there is a small neighborhood U of the 1-source-sink point on which V and its small perturbation are identical. Hence it suffices to show that any small perturbation \tilde{V} of $V|_{\mathcal{D}_\zeta(M) \setminus U}$ which fixes ∂U is topological equivalence to $V|_{\mathcal{D}_\zeta(M) \setminus U}$. Since the streamlines in the neighborhood of the 1-source-sink point can be obtained from the streamlines around two centers by identifying the centers as we have discussed in Figure 6, we can replace $V|_U$ with some vector field on U with two centers. Then all ss-(∂ -)saddle connections are replaced by (∂ -)saddle connections. By Theorem 3.1, the resulting vector field of V are structurally stable. Hence \tilde{V} is topological equivalent to $V|_{\mathcal{D}_\zeta(M) \setminus U}$. \square

It follows from Theorem 3.2 that any structurally stable Hamiltonian vector field with the 1-source-sink point is determined by the union of saddle connections, ∂ -saddle connections, ss-saddle connections and ss- ∂ -saddle connections up to topological equivalence, which is called *the ss-saddle connection diagram*. While all of the operations can be applied to the initial pattern I , the operation A_2 is not allowed for the initial pattern II , which is proved as follows.

Lemma 3.2. *The structurally stable Hamiltonian vector field V with the 1-source-sink point can be represented by either a sequence $IO_1 \cdots O_k$ or a sequence $II\tilde{O}_1 \cdots \tilde{O}_k$ where $O_i \in \{A_0, A_2, B_0, B_2, C\}$ and $\tilde{O}_i \in \{A_0, B_0, B_2, C\}$ for $i = 1, \dots, k$.*

Proof. Let us first replace the 1-source-sink point with two centers as in the proof of Theorem 3.2. Then the resulting vector field belongs to $V \in \mathcal{H}^r$ and thus it is represented by an O -word, say, $O\tilde{O}_1 \cdots \tilde{O}_{k+1}$ with $\tilde{O}_i \in \{B_0, B_2, C\}$ for $i \geq 2$. Now we recover the 1-source-sink point by collapsing the two centers again. Then the header of the O -word becomes $OB_2 = I$ or $OB_0 = II$ as we have discussed in Figure 6, and the other words \tilde{O}_i change to either A_0, A_2, B_0, B_2 , or C for $i \geq 2$. Moreover, if we operate A_2 to II at some step, then the 1-source-sink point has ∂ -saddles and so V can be constructed from IA_0 as we have already confirmed with the identity $IA_0 = IIA_2$ in Figure 4. \square

The proof of this lemma indicates that the difference in the patterns I and II originates from the fact that there are two topologically different O -words, which are OB_0 and OB_2 , in $\mathcal{D}_\zeta(1)$. Hence, we can assign a sequence of the operations, $IO_1O_2 \cdots O_k$ with $O_i \in \{A_0, A_2, B_0, B_2, C\}$ and $II\tilde{O}_1\tilde{O}_2 \cdots \tilde{O}_k$ with $\tilde{O}_i \in \{A_0, B_0, B_2, C\}$ for $i \leq k$ to represent the structurally stable streamline patterns starting from I and II respectively. In the sequence of operations from I , A_0 or C should appear before B_0 and B_2 , since there contains no closed orbit in the initial pattern I to which B_0 and B_2 are applied. This fact is stated as follows.

Lemma 3.3. *Let $IO_1 \cdots O_k$ be a sequence of operations, where $O_i \in \{A_0, A_2, B_0, B_2, C\}$ for $i = 1, \dots, k$. Then the followings are equivalent.*

- 1) *The sequence is a word representation for a structurally stable Hamiltonian vector with the 1-source-sink point in $\mathcal{D}_\zeta(M)$.*
- 2) *For any $i > 1$ with $O_i = B_0$ or B_2 , there is some $j < i$ such that $O_j = A_0$ or C .*

Regrading a sequence of operations from II , B_2 should be followed by C , which is given as follows.

Lemma 3.4. *Let $II\tilde{O}_1 \cdots \tilde{O}_k$ be a sequence of operations, where $\tilde{O}_i \in \{A_0, B_0, B_2, C\}$ for $i = 1, \dots, k$. Then the followings are equivalent.*

- 1) *The sequence is a word representation for a structurally stable vector field with the 1-source-sink point in $\mathcal{D}_\zeta(M)$.*
- 2) *For any $i > 1$ with $\tilde{O}_i = C$, there is some $j < i$ such that $\tilde{O}_j = B_2$.*

We refer to the sequence of words for a given structurally stable vector field with the 1-source-sink point from I and II as a I -word and a II -word respectively. A word can be assigned for a structurally stable streamline pattern as a sequence of operations. However, we must notice that there are many streamline patterns represented by one word. For example, in the initial pattern II , ss-orbits exist above and below the 1-source-sink point to both of which A_0 is applied, which gives rise to different streamline patterns represented by IIA_0 . On the other hand, we also notice that there are several word representations for one structurally stable streamline pattern. Indeed, the words IA_0A_2 and IA_2A_0 represent the same streamline patterns. Based on these observation, it is useful to discuss the commutativity of the operations in the sequence. Obviously the same operations commute. The commutativity of A_0 and C for I -words and II -words are shown as follows.

Lemma 3.5. *The streamline patterns with the word representations $O_0O_1 \cdots O_iA_0CO_{i+3} \cdots O_k$ and $O_0O_1 \cdots O_iCA_0O_{i+3} \cdots O_k$ with $O_0 \in \{I, II\}$ are equivalent. Namely, A_0 and C commute in the word representation.*

Proof. Since A_0 does not increase boundaries with ∂ -saddles and C just changes a boundary with ∂ -saddles, these operations are applied independently. \square

The operation A_2 commutes with A_0, B_0 and B_2 for I -words.

Lemma 3.6. *The streamline patterns with the word representations $IO_1 \cdots O_iA_2O_{i+2} \cdots O_k$ and $IO_1 \cdots A_2O_iO_{i+2} \cdots O_k$ with $O_i \in \{A_0, B_0, B_2\}$ are equivalent.*

Proof. Since A_0 and A_2 are applied to different ss-orbits, A_0 and A_2 commute. The operation A_2 increases no closed orbits to which B_0 and B_2 are applied. Conversely, B_0 and B_2 add no ss-orbits. Hence B_0 and B_2 commute with A_2 . \square

	A_0	A_2	B_0	B_2	C
A_0	=	=	\leq	\leq	=
A_2		=	=	=	\leq
B_0			=	\leq	\geq
B_2				=	\parallel
C					=

Table 1: Commutativity between the five operations.

The equivalence between the streamline patterns with respect to the exchange of operations in the sequence proven in the above lemmas are symbolically denoted by $A_0C = CA_0$, $A_2A_0 = A_0A_2$, $A_2B_0 = B_0A_2$ and $A_2B_2 = B_2A_2$. In order to discuss the commutativity for the other operations, we need to define an inclusion relation between two word representations. If the streamline patterns represented by a word $O_0O_1 \cdots O_{i-1}O_iO_{i+1}O_{i+2} \cdots O_k$ are included by those by a word $O_0O_1 \cdots O_{i-1}O_{i+1}O_iO_{i+2} \cdots O_k$, then the inclusion relation is symbolized by $O_iO_{i+1} \leq O_{i+1}O_i$. Then we have the following inclusion relations.

Lemma 3.7. *The inclusion relations $B_0A_0 \leq A_0B_0$, $B_2A_0 \leq A_0B_2$, $CA_2 \leq A_2C$, $B_2B_0 \leq B_0B_2$, $B_0C \leq CB_0$ hold for the exchange of two operations in the sequence.*

Proof. First, A_0 is independently applied to an ss-orbit, even if B_0 and B_2 exist in the sequence before A_0 . On the other hand, A_0 adds new closed orbits to which B_0 and B_2 are applied. Hence, we have $B_0A_0 \leq A_0B_0$ and $B_2A_0 \leq A_0B_2$. Second, C does not affect A_2 , since C creates no new ss-orbits. Conversely, A_2 adds a new boundary with two ∂ -saddles to which C can be applied. Thus $CA_2 \leq A_2C$ holds. Third, B_0 increases new closed orbits to which B_2 is applied, but B_2 does not. Hence, we have $B_2B_0 \leq B_0B_2$. Finally, $CB_0 \geq B_0C$ holds, since C increases new closed orbits and B_0 adds no boundary with ∂ -saddles. \square

Note that we cannot determine the inclusion relation for exchange of B_2 and C in the sequence of word representations, which is symbolized by $B_2C \parallel CB_2$. The commutativity of the five operations in word representations and their inclusion relations are summarized in Table 1. Owing to the order relation \leq , we can show the existence of a maximal word for any structurally stable streamline patterns.

Lemma 3.8. *Each structurally stable streamline pattern on $\mathcal{D}_\zeta(M)$ has a maximal word representation.*

Proof. Notice that the relation \leq implies that the reflexive and transitive relation on the set of O -words (resp. I -words, II -words). Since the number of O -words (resp. I -words, II -words) is finite, each word is less than or equal to some maximal word. \square

Let us note that this lemma concludes nothing about the uniqueness of the maximal word representation. As a matter of fact, the expression of the maximal word depends on how we exchange the words in the sequence following the rules in Table 1. Hence, we need to specify how to exchange the words in order to obtain the unique expression of the maximal word representation. Thus, in the rest of this section, we derive canonical expressions for maximal O -words, I -words and II -words. Let us define a block component $W(s, t, u)$ by $W(s, t, u) = (B_0)^s (B_2)^t (C)^u$ for non-negative integers s, t and u . Then we have the following theorem.

Theorem 3.3. *For any maximal O -word for a structurally stable streamline pattern in $\mathcal{D}_\zeta(M)$, there exist integers $k \geq 1$, $s_m, t_m \geq 0$ for $m = 1, \dots, k$ and $u_m > 0$ for $m = 1, \dots, k-1$ such that it is expressed by*

$$OW(s_1, t_1, u_1) \cdots W(s_{k-1}, t_{k-1}, u_{k-1})W(s_k, t_k, 0), \quad (2)$$

where $t_m > 0$ for any $m < k$ with $M = 1 + \sum_{m=1}^{k-1} (s_m + t_m + u_m) + s_k + t_k$.

Proof. Let us first note that it is unable to exchange B_0C and B_2C in the sequence of any O -word to obtain its maximal O -word owing to $B_2C \parallel CB_2$ and $B_0C \geq CB_0$. We show that every O -word assigned to

the structurally stable streamline pattern in $\mathcal{D}_\zeta(M)$ can be reduced to the maximal O -word inductively as follows.

Starting the initial word O , we look for the location where $(C)^{u_1}$ first appears in the sequence of the O -word. If there exists no operation C in the sequence, i.e., $u_1 = 0$, then the O -word consist of B_0 and B_2 and thus it can be reduced to $O(B_0)^{s_1}(B_2)^{s_2} = OW(s_1, t_1, 0)$ for some $s_1, t_1 \geq 0$ by exchanging B_0 and B_2 owing to $B_2B_0 \leq B_0B_2$, which ends the proof. On the other hand, if $u_1 \neq 0$, we can rearrange the sequence with B_0 and B_2 between O and $(C)^{u_1}$ by the block component $W(s_1, t_1, u_1)$ for some $t_1 > 0$. This is because if $t_1 = 0$ we have $O(B_0)^{s_1}(C)^{u_1} \dots \geq O(C)^{u_1}(B_0)^{s_1} \dots$ owing to $(B_0)^{s_1}(C)^{u_1} \geq (C)^{u_1}(B_0)^{s_1}$, which is not an O -word. Hence, the O -word is expressed as $OW(s_1, t_1, u_1) \dots$ with $t_1, u_1 > 0$.

Now suppose that $u_m \neq 0$ and the O -word is reduced to $OW(s_1, t_1, u_1) \dots W(s_m, t_m, u_m) \dots$ with $t_i > 0$ for any $i \leq m$. Then we look for the location of $(C)^{u_{m+1}}$ in the sequence beyond $W(s_m, t_m, u_m)$. If $u_{m+1} = 0$, then the O -word can be reduced to

$$OW(s_1, t_1, u_1) \dots W(s_m, t_m, u_m)W(s_{m+1}, t_{m+1}, 0)$$

for some $s_{m+1}, t_{m+1} \geq 0$ by exchanging B_0 and B_2 , which finishes the proof. Otherwise the sequence of B_0 and B_2 between $W(s_m, t_m, u_m)$ and $(C)^{u_{m+1}}$ is reduced to the block component $W(s_{m+1}, t_{m+1}, u_{m+1})$ for some $s_{m+1} \geq 0$ and $t_{m+1} > 0$. The positivity of t_{m+1} is assured as follows. If $t_{m+1} = 0$, we have

$$\begin{aligned} & OW(s_1, t_1, u_1) \dots W(s_m, t_m, u_m)(B_0)^{s_{m+1}}(C)^{u_{m+1}} \dots \\ & \leq OW(s_1, t_1, u_1) \dots W(s_m, t_m, u_m + u_{m+1})(B_0)^{s_{m+1}} \dots \end{aligned}$$

owing to $B_0C \leq CB_0$. Then with $\tilde{u}_m = u_m + u_{m+1}$, the sequence is reduced to

$$OW(s_1, t_1, u_1) \dots W(s_m, t_m, \tilde{u}_m) \dots ,$$

for which we can repeat the process again. \square

Theorem 3.4. *Let p, q, r be non-negative integers. Then, for any maximal I -word for a structurally stable streamline pattern in $\mathcal{D}_\zeta(M)$, there exist integers $k \geq 1$, $s_m, t_m \geq 0$ for $m = 1, \dots, k$ and $u_m > 0$ for $m = 1, \dots, k - 1$ such that it is expressed by*

$$I(A_0)^p(A_2)^q(C)^rW(s_1, t_1, u_1) \dots W(s_{k-1}, t_{k-1}, u_{k-1})W(s_k, t_k, 0), \quad (3)$$

where $t_m > 0$ for any $m < k$ with $M = p + q + r + \sum_{m=1}^{k-1}(s_m + t_m + u_m) + s_k + t_k$, if $p + r > 0$. Otherwise it is represented by $I(A_2)^q$ with $M = q$.

Proof. For a given I -word representing a structurally stable streamline pattern in $\mathcal{D}_\zeta(M)$, we can move all A_0 and A_2 in the sequence of operations before B_0 , B_2 and C by exchanging the order of the operations owing to $A_0A_2 = A_2A_0$, $CA_2 \leq A_2C$, $B_2A_2 = A_2B_2$, $B_0A_2 = A_2B_0$, $CA_0 = A_0C$, $B_0A_0 \leq A_0B_0$ and $B_2A_0 \leq A_0B_2$. Hence, the I -word is reduced to $I(A_0)^p(A_2)^qO_{p+q+1} \dots O_M$ for some $p, q \geq 0$, in which $O_i \in \{B_0, B_2, C\}$ for $p + q < i \leq M$.

Suppose first that $p = 0$. If $O_{q+1} \neq C$, namely $r = 0$, then there contains no B_0 and B_2 in the following sequence, since they cannot be applied without A_0 or C in the sequence of I -words due to Lemma 3.3. Hence, if $p + r = 0$, the I -word is represented by $I(A_2)^q$ and $M = q$. On the other hand, if $O_{q+1} = C$, then there exists $r > 0$ such that the I -word is represented by $I(A_2)^q(C)^rO_{q+r+1} \dots O_M$ in which $O_i \in \{B_0, B_2, C\}$ for $q + r < i \leq M$. The remaining sequence $O_{q+r+1} \dots O_M$ can be reduced to some block components of B_0 , B_2 and C with using the same procedure as for O -words in Theorem 3.3. That is to say, there exist integers $k \geq 1$, $s_m, t_m \geq 0$ for $m = 1, \dots, k$ and $u_m > 0$ for $m = 1, \dots, k - 1$ such that the I -word is expressed by

$$I(A_2)^q(C)^rW(s_1, t_1, u_1) \dots W(s_{k-1}, t_{k-1}, u_{k-1})W(s_k, t_k, 0),$$

where $t_m > 0$ for any $m < k$. This is the maximal expression for the I -word for $p = 0$ and $r > 0$.

Next we assume $p \neq 0$. Then B_0 and B_2 can exist in the remaining part of the sequence $I(A_0)^p(A_2)^q \dots$ to which we can apply the same procedure for the remaining sequence of B_0 , B_2 and C as used for O -words. Hence, we have the maximal expression (3). \square

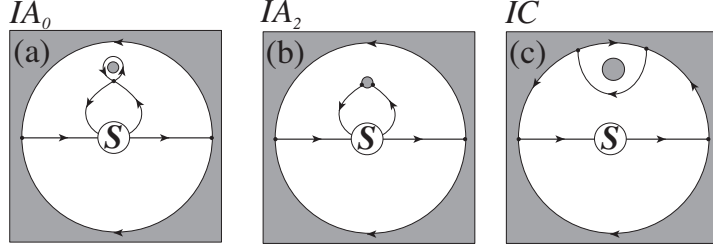


Figure 7: Catalogue of ss-saddle connection diagrams in $\mathcal{D}_\zeta(1)$ and their maximal I -words.

Theorem 3.5. *Let p be a non-negative integer. Then, for any maximal II -word for a structurally stable streamline pattern in $\mathcal{D}_\zeta(M)$, there exist integers $k \geq 1$, $s_m, t_m \geq 0$ for $m = 1, \dots, k$ and $u_m > 0$ for $m = 1, \dots, k - 1$ such that it is expressed by*

$$II(A_0)^p W(s_1, t_1, u_1) \cdots W(s_{k-1}, t_{k-1}, u_{k-1}) W(s_k, t_k, 0), \quad (4)$$

where $t_m > 0$ for any $m < k$ with $M = p + \sum_{m=1}^{k-1} (s_m + t_m + u_m) + s_k + t_k$.

Proof. The proof is done similarly as in Theorem 3.4, since Lemma 3.4 indicates that II -words have the same rule as O -words in terms of the order of operations B_0 , B_2 and C in the sequence. \square

4 Structurally stable streamline patterns in $\mathcal{D}_\zeta(1)$ and $\mathcal{D}_\zeta(2)$

We give all possible streamline patterns for the vortex flows in the presence of the uniform flow in $\mathcal{D}_\zeta(1)$ and $\mathcal{D}_\zeta(2)$ and their corresponding maximal word representations with using (2), (3) and (4). In order to obtain the canonical expressions, we need to determine the indices p , q , r , the number of the block components k and its corresponding integers s_m , t_m for $m = 1, \dots, k$ and u_m for $m = 1, \dots, k - 1$ in the combinatorial way. Let us note that the number of the block components k satisfies $2(k - 1) \leq M$ for I -words and II -words, and $2(k - 1) \leq M - 1$ for O -words, since we have $u_m = t_m = 1$ for $1 \leq m \leq k - 1$ at least.

First, we consider all maximal O -words. Since $M = 1 + \sum_{m=1}^{k-1} (s_m + t_m + u_m) + s_k + t_k$ according to Theorem 3.3, the maximal O -word for $M = 1$ is O . When $M = 2$ we have $k = 1$ and thus we determine the combinations of the indices (s_1, t_1) in the block component. Since we have $(s_1, t_1) = (1, 0)$ and $(0, 1)$, the maximal O -words for $M = 2$ are OB_0 and OB_2 whose corresponding streamline patterns have already been shown in Figure 6(a) and (c).

For maximal I -words, since $M = p + q + r + \sum_{m=1}^{k-1} (s_m + t_m + u_m) + s_k + t_k$ by Theorem 3.4, $k = 1$ is allowed for $M = 1$. When $p = r = 0$, we have $q = 1$, whose maximal I -word becomes IA_2 . If $p + r > 0$, we have either $p = 1$ or $r = 1$. Hence the maximal I -words for $M = 1$ are given by IA_0 , IA_2 and IC whose corresponding streamline patterns are shown in Figure 7. For $M = 2$, if $k = 2$, then we have $t_1 = u_1 = 1$ and thus $p = r = 0$ due to $M = 2$. However, if $p = r = 0$, then we have $s_1 = t_1 = 0$, which is a contradiction. Hence, we have $k = 1$ and thus we distribute $M = 2$ to the set of the indices (p, q, r, s_1, t_1) . First, when $p = r = 0$, we have the maximal I -word IA_2A_2 for $q = 2$. There are two streamline patterns represented by IA_2A_2 , since ss-orbits to which A_2 is applied exist in the two disjoint regions separated by the ss- ∂ -saddle connections. If we apply A_2 to two ss-orbits on the different regions, the streamline pattern for IA_2A_2 becomes Figure 8(a). Applying A_2 to two ss-orbits on the same side, we obtain the other streamline pattern represented by IA_2A_2 as shown in Figure 8(b).

When $p + r > 0$, the combinations of the indices (p, q, r, s_1, t_1) and their corresponding maximal I -words are listed in Table 2 whose representing streamline patterns are shown in Figure 8 and Figure 9. There are several two streamline patterns represented by IA_0A_0 , see Figure 8(c) and (d), depending on whether or not A_0 are applied to an ss-orbit on the same side where the saddle created by A_0 is located. Regarding IA_0A_2 , there are three kinds of different streamline pattern denoted by IA_0A_2 shown in Figure 8(e)–(g), since A_2 can be applied to an ss-orbit outside or inside of the saddle created by A_0 . Figure 8(h) and

p	q	r	s_1	t_1	I -word
2	0	0	0	0	IA_0A_0
1	1	0	0	0	IA_0A_2
1	0	1	0	0	IA_0C
1	0	0	1	0	IA_0B_0
1	0	0	0	1	IA_0B_2
0	1	1	0	0	IA_2C
0	0	1	1	0	ICB_0
0	0	1	0	1	ICB_2
0	0	2	0	0	ICC

Table 2: Combinations of the indices in the maximal I -words for $M = 2$ with $p + r > 0$ and their corresponding maximal I -word representations.

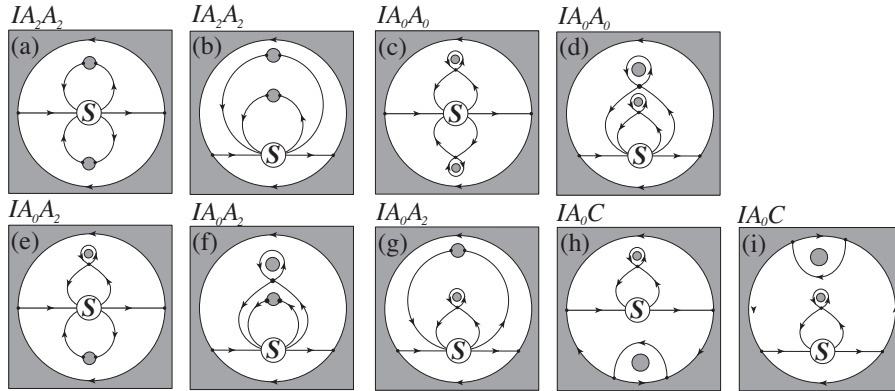


Figure 8: Catalogue of ss-saddle connection diagrams in $\mathcal{D}_c(2)$ and their maximal I -words.

(i) show the streamline patterns represented by IA_0C , which correspond to the cases when we apply the operation C to a boundary with ∂ -saddles on the same side where the saddle created by A_0 is located or on the different sides. Since there is only one region in IA_0 that contains closed orbits to which B_0 and B_2 are applied, each of IA_0B_0 and IA_0B_2 represents one streamline pattern whose corresponding ss-saddle connection diagrams are shown in Figure 9(a) and (b) respectively. For IA_2C , we obtain two streamline patterns when we apply C to a boundary with two ∂ -saddles on the different sides (Figure 9(c)) or on the same side (Figure 9(d)) of the the boundary created by A_2 . The maximal I -words ICB_0 and ICB_2 represent streamline patterns shown in Figure 9(e) and (f) respectively, since the B_0 and B_2 are applied to a closed orbit around the boundary created by C . We have three streamline patterns for ICC in which two ∂ -saddle connections are on the different sides (Figure 9(g)), they are on the same side (Figure 9(h)) and one ∂ -saddle-connection encloses the other ∂ -saddle-connection (Figure 9(i)).

Finally we consider the maximal II -words in $\mathcal{D}_c(1)$ and $\mathcal{D}_c(2)$. Owing to $k = 1$ for $M = 1$, we have three combinations of the indices $(p, s_1, t_1) = (1, 0, 0)$, $(0, 1, 0)$ and $(0, 0, 1)$ whose corresponding maximal II -words are IIA_0 , IIB_0 and IIB_2 whose corresponding ss-saddle connection diagrams are shown in Figure 10(a)–(b), (c) and (d) respectively. There are two patterns for IIA_0 , since the initial pattern II have two disjoint regions containing ss-orbits to which A_0 is applied.

Now suppose that $M = 2$. When the number of the block components is $k = 2$, we have only one maximal II -word IIB_2C for $t_1 = u_1 = 1$ whose representing streamline pattern is given in Figure 12(g). For $k = 1$, Table 3 is the list of the combinations of the indices (p, s_1, t_1) and their word representations. All streamline patterns represented by the maximal II -words are drawn in Figure 11 and Figure 12. Since ss-orbits exist in the two disjoint regions in the pattern II , we obtain three streamline patterns when we apply the operations A_0A_0 in the different regions (Figure 11(a)) and in the same region (Figure 11(b) and

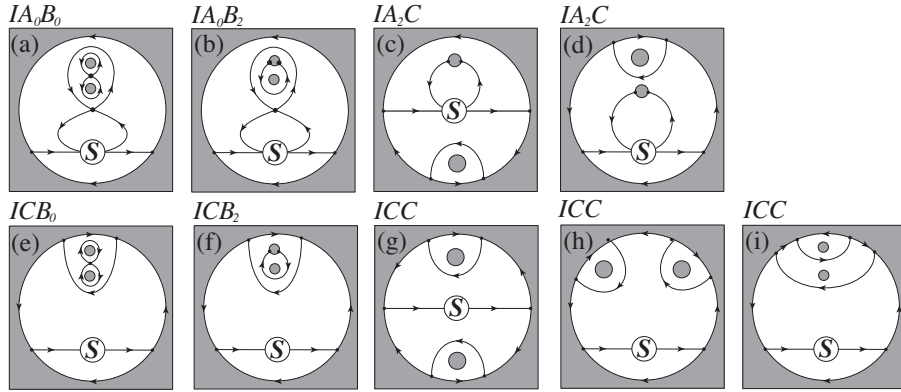


Figure 9: Catalogue of ss-saddle connection diagrams in $\mathcal{D}_c(2)$ and their maximal I -words. (continued)

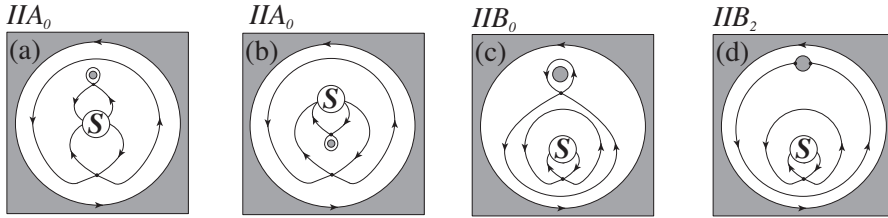


Figure 10: Catalogue of ss-saddle connection diagrams in $\mathcal{D}_c(1)$ and their maximal II -words.

p	s_1	t_1	II -word
2	0	0	IIA_0A_0
1	1	0	IIA_0B_0
1	0	1	IIA_0B_2
0	2	0	IIB_0B_0
0	1	1	IIB_0B_2
0	0	2	IIB_2B_2

Table 3: Combinations of the indices in the maximal I -words for $M = 2$ if $p+r > 0$ and their corresponding maximal I -word representations.

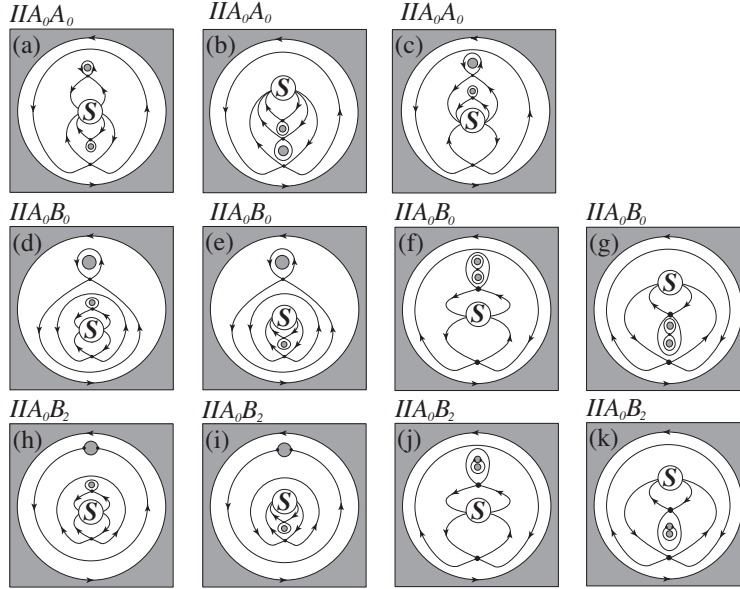


Figure 11: Catalogue of ss-saddle connection diagrams in $\mathcal{D}_c(2)$ and their II -words.

(c). On the other hand, as shown in Figure 10(a) and (b), IIA_0 represents the two streamline patterns that have two disjoint regions containing closed orbits to which we can apply B_0 and B_2 . Hence, we have four streamline patterns for IIA_0B_0 shown in Figure 11(d)–(g) and IIA_0B_2 shown in Figure 11(h)–(k). Since IIB_0 has three disjoint regions with closed orbits to which we can apply B_0 and B_2 , we have three streamline patterns for IIB_0B_0 and IIB_0B_2 . However, regarding IIB_0B_0 , two of them have the same topology, IIB_0B_0 represents two streamline patterns. Thus all ss-saddle connection diagrams for IIB_0B_0 and IIB_0B_2 are shown in Figure 12(a)–(b) and Figure 12(c)–(e) respectively. The maximal II -word IIB_2B_2 represents one streamline pattern in Figure 12(f). The maximal II -word IIB_2B_2 represents one streamline pattern in Figure 12(g).

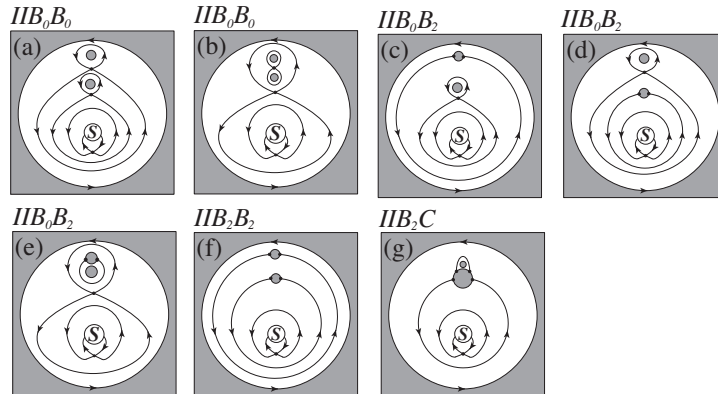


Figure 12: Catalogue of ss-saddle connection diagrams in $\mathcal{D}_c(2)$ and their II -words.

5 Summary and discussion

This paper has provided how to assign a sequence of words, called the maximal word, to every structurally stable streamline patterns generated by the potential flows consisting of the uniform flow and point vortices in two-dimensional multiply connected domains. Owing to the maximal word representation, we not only classify the structurally stable streamline topologies, but we also make a complete catalogue of all possible streamline patterns in a combinatorial manner. Let us note that the canonical expressions of the maximal words (2), (3) and (4) represent a family of streamline patterns. On the other hand, for a sequence of words assigned to every streamline pattern, we can convert it uniquely into a canonical maximal word representation following the procedures given in the proof of Theorem 3.3, 3.4 and 3.5.

The classification of the streamline patterns for the vortex flows with the uniform flow is an extension of the preceding works by Aref and Brøns[1]. As a matter of fact, the maximal O -words can represent the structurally stable streamline patterns without the uniform flow in the unbounded plane when we regard circular boundaries as point vortices. Since there is no circular boundary, the operations B_2 and C are not allowed. Hence, the maximal O -words for the streamline pattern becomes OB_0^q for some $q \geq 0$. Let us note that Aref and Brøns have considered the structurally unstable patterns that contains heteroclinic connections between saddles, which cannot be represented by the maximal O -words. Furthermore, the maximal word representations of the structurally stable streamline patterns add the following new aspects to the preceding work that are of significance from the application point of view. First, one can obtain all possible streamline patterns with their maximal word representations in multiply connected exterior domains in the presence of the uniform flow, which are applicable to the classification of the flow patterns arising in biofluids and environmental flows. Second, we pay attention to the structurally stable flows, which are more probable to be observed in real fluid problems.

In the (ss-)saddle connection diagrams shown in this paper, all obstacles contained in the multiply connected domain $\mathcal{D}_\zeta(M)$ are represented by M circular holes. However, these circular obstacles can be replaced by point vortices and elliptic stagnation points, since they generate closed circular orbits around them that are topologically equivalent to each other. Thus, the genus M of the domain $\mathcal{D}_\zeta(M)$ is equivalent to the sum of the numbers of circular holes, point vortices and elliptic centers. Let us also note that the topological classification of the streamline patterns is independent of the shapes of the boundary of the obstacles, since the complex potentials are conformally invariant under the action of the conformal mapping between any multiply connected domains and canonical circular domains with the same multiplicity.

Let us finally note that it is important to consider structurally unstable streamline patterns that contain heteroclinic orbits and multiple homoclinic saddle connections and so on. Since the structurally unstable streamline patterns are reduced to some structurally stable ones under small perturbations, these unstable streamline pattern is regarded as a marginal state between two stable streamline patterns with the maximal word representations. Consequently, through the unstable streamline patterns, we can describe the transition between two maximal words in a combinatorial way, which will be reported in near future.

References

- [1] AREF, H. & BRØNS, M. 1998 On stagnation points and streamline topology in vortex flows. *J. Fluid Mech.* **370**, 1–27.
- [2] BAKER, H. 1995 Abelian Functions, Cambridge Univ. Press, Cambridge.
- [3] CROWDY, D. 2006 Calculating the lift on a finite stack of cylindrical aerofoils. *Proc. Roy. Soc. A* **462**, 1387–1407.
- [4] CROWDY, D. & MARSHALL, J. 2005 Analytical formulae for the Kirchhoff-Routh path function in multiply connected domains. *Proc. Roy. Soc. A* **461**, 2477–2501.
- [5] CROWDY, D. G. & MARSHALL, J. S. 2007 Computing the Schottky-Klein prime function on the Schottky double of planar domains, *Comput. Methods Funct. Theory* **7**, 293–308.
- [6] IIMA, M. & YANAGITA, T. 2001 Is a two-dimensional butterfly able to fly by symmetric flapping? *J. Phys. Soc. Japan* **70**, 5–8.

- [7] JOHNSON, E. R. & McDONALD, N. R. 2004 The motion of a vortex near two circular cylinders. *Proc. Roy. Soc. A* **460**, 939–954.
- [8] JOHNSON, E. R. & McDONALD, N. R. 2005 Vortices near barriers with multiple gaps. *J. Fluid Mech.* **531**, 335–358.
- [9] KLEIN, K. 1890 Zur Theorie der Abelschen Functionen. *Math. Ann.* **36**, 1–83.
- [10] KIDAMBI, R. & NEWTON, P. K. 2000 Streamline topologies for integrable vortex motion on a sphere. *Physica D* **140**, 95–125.
- [11] LENTINK, D., DICKSON, W. B., VAN LEEUWEN, J. L. & DICKINSON, M. H. 2009 Leading-edge vortices elevate lift of autorotating plant seeds. *Science* **324**, 1438–1440.
- [12] MA, T & WANG, S 2005 Geometric theory of incompressible flows with applications to fluid dynamics. *Mathematical Surveys and Monographs* **119**, American Mathematical Society, Providence, RI.